Spanwise bifurcation in plane-symmetric sudden-expansion flows

T. P. Chiang,[1] Tony W. H. Sheu,[1] Robert R. Hwang,[2,*] and A. Sau[2]
[1]*Department of Naval Architecture and Ocean Engineering, National Taiwan University, Taipei, Taiwan, Republic of China*
[2]*Institute of Physics, Academia Sinica, Taipei, Taiwan, Republic of China*
(Received 29 May 2001; published 19 December 2001)

Present computational investigation reports a steady bifurcation phenomenon for three-dimensional flows through a plane-symmetric sudden expansion. When the channel aspect ratio exceeds a critical value, the well-known step height (pitchfork) bifurcation evolves with different symmetry breaking orientations on the left and right sides of the channel and bifurcates in the spanwise direction. For the channel aspect ratio less than the critical value, the originally occurring spanwise bifurcation cannot be stably retained and evolves eventually to a step height bifurcation. Compared to step height bifurcation, the spanwise bifurcation is found to be more difficult to obtain, because the symmetric flow present on the spanwise symmetry plane is unstable in two dimensions. For completeness, an extensive analysis of the observed spanwise bifurcation, covering its transient behavior, dependence on flow Reynolds number, channel aspect ratio, and expansion ratio, is included.

DOI: 10.1103/PhysRevE.65.016306 PACS number(s): 47.15.Fe, 47.20.Ky, 47.60.+i, 83.85.Pt

I. INTRODUCTION

Laminar flow of an incompressible, Newtonian fluid in a channel with sudden expansion has been the subject of many previous investigations. The inherent nonlinear flow transition from symmetric states to asymmetric equilibrium states with increased Reynolds number in such a simple geometry makes the problem attractive and serves as a first step towards understanding of a more complex three-dimensional flow separation usually encountered in many engineering applications. Experimental investigation into this problem has been quite plentiful, and we cite a small selection of the literature here, namely the works of Macagno and Hung [1], Durst *et al.* [2], Cherdron *et al.* [3], Sobey [4], Latornell and Pollard [5], Sobey and Drazin [6], Fearn *et al.* [7], and Durst *et al.* [8]. These experimental studies have reported that an initially symmetric flow in a channel with sudden expansion about its center line can become asymmetric as the Reynolds number Re is increased beyond a critical value. In the literature, such a symmetry breaking flow phenomenon in symmetric channels is termed as Coanda effect [9]. The symmetry breaking phenomenon has been well recognized as being influenced by the expansion ratio, E, and the aspect ratio, A, of the channel [3].

As the flow loses its stability to asymmetric and bifurcated flows, the increased velocity near one wall can cause the pressure to decrease near that wall. It is argued that this pressure gradient can sustain flow asymmetry in the symmetric channel. Cherdron *et al.* [3] attributed these instabilities to step corner disturbances, which can be amplified due to the presence of the shear layer. Sobey [4] experimentally confirmed the asymmetric disturbance, configured in a vortex sheet. The already asymmetric flows, which are considered to be two-dimensional except for boundary layers on the sidewall, may evolve and exhibit unsteady behavior and consequently three-dimensional effects will be more prominent at a sufficiently higher Reynolds number. Such a flow finally develops into a fully turbulent asymmetric flow when the Reynolds number is further increased. The onset of flow asymmetry is closely tied up with flow bifurcation and instabilities. Linear stability analysis is a classical theory used to study the pitchfork bifurcation. Before becoming fully turbulent the flow may evolve first into a time periodic Hopf bifurcation [6]. Under certain circumstances, such a bifurcation can cause a direct entry into oscillating flow motion, without going through the intermediate pitchfork bifurcation [10]. This type of shear instability is often accompanied by Tollmein-Schlichting waves, which are associated with kelvin-Helmholtz instability. In this study, we shall confine ourselves to Reynolds numbers that permit only pitchfork bifurcation, and have no intention to deal with the growth-shedding-decaying flow dynamics.

Apart from experimental studies on this problem, there exist numerous computational investigations for suddenly expanded flows. Most of the previous Navier-Stokes analyses have been carried out in two dimensions. Herewith, we cite some published papers, which may provide adequate material on the topic. A comprehensive review of the previous works [6–8,10–13] has been presented by Drikakis [14], where information on comparison between numerical and experimental data, investigation of the effect of channel expansion ratio, and determination of critical Reynolds number are provided. Alleborn *et al.* [15] applied the continuation method to study the bifurcation structure and extended the bifurcation picture by computing additional solution branches and bifurcation points. Fearn *et al.* [7] and Durst *et al.* [8] suspected that a slight asymmetry (1%) in the channel geometry could be responsible for the flow asymmetry and bifurcation. Recently, Hawa and Rusak [16] found that a small asymmetry in the channel expansion changes the pitchfork bifurcation into two separate branches of equilibrium states. Hawa and Rusak [17] also provided a physical mechanism to explain the transition from symmetric to asymmetric

*Author to whom correspondence should be addressed at Institute of Physics, Academia Sinica, Taipei, Taiwan, ROC. FAX: 886-2-27834187. Email address: phhwang@ccvax.sinica.edu.tw

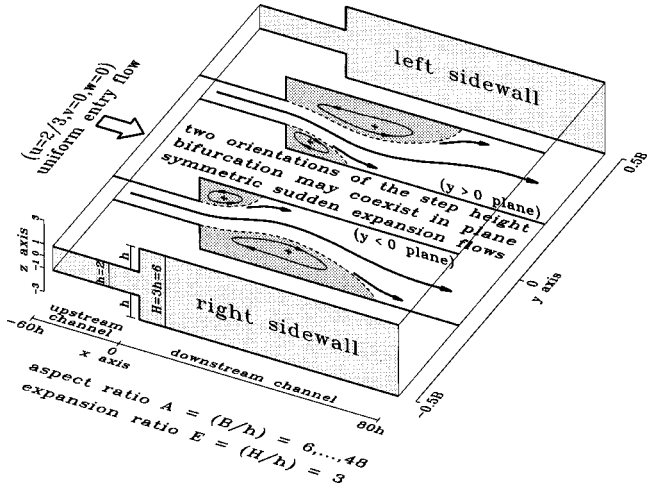

FIG. 1. The geometry and flow condition for the three-dimensional analysis of the flow in a plane-symmetric channel with sudden expansion ratio $E=3$.

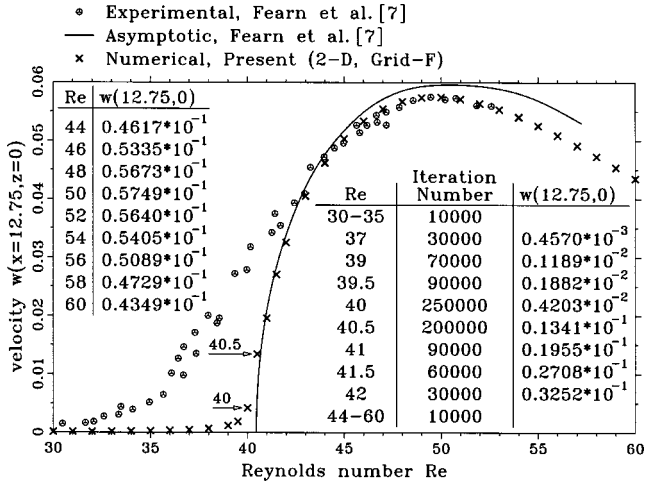

FIG. 2. Comparison of bifurcation diagram, based on the velocity component $w(x=12.75,z=0)$ for the case of $E=3$, with the numerical and experimental data of Fearn *et al.* [7].

states and demonstrate the various possibilities of the evolution of disturbances. These computational studies could predict the general trends of previous experimental observations. Recent progress in the development of high speed computing technique has provided a new impetus for large size flow simulation. This makes three-dimensional Navier-Stokes flow simulations possible [18–20] and enables us to examine suddenly expanded flow under the influence of end wall effect. In addition, the flow shows an increasingly evident three-dimensional nature with increasing Reynolds number. At a higher Reynolds number, the observed three-dimensional effects lead to flow unsteadiness [2–4,7,21]. Thus the modeling of flows in the third dimension becomes indispensable. On the other hand, two-dimensional assumption in the numerical investigations into the suddenly expanded flow has been experimentally confirmed to be inappropriate [8].

In a recent computational study Chiang *et al.* [22] ad-

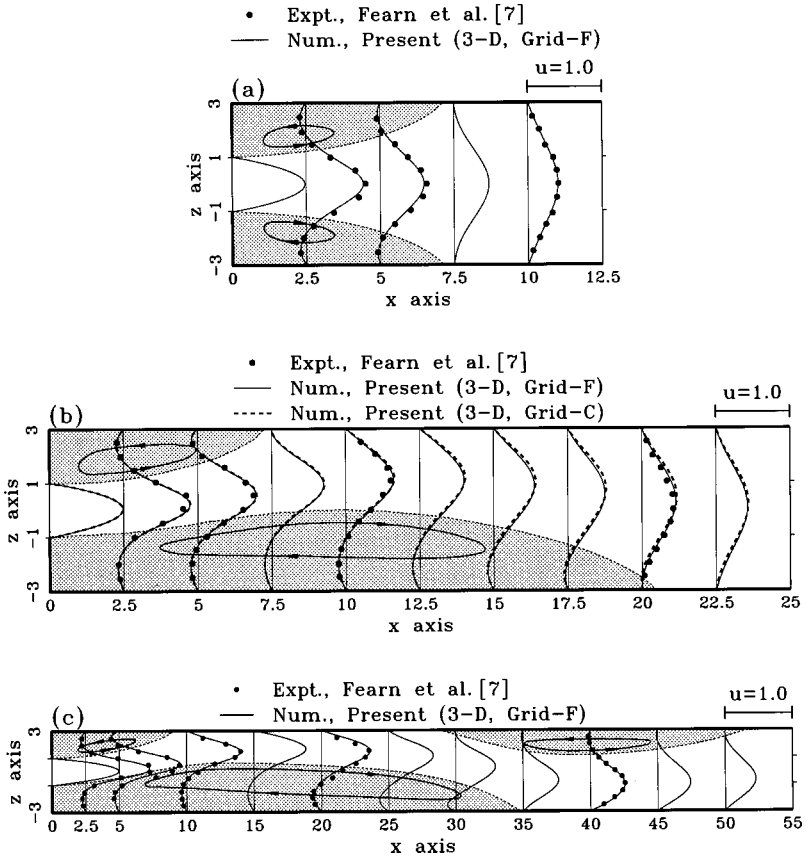

FIG. 3. Comparison of u velocity distribution, at different streamwise locations of the plane of symmetry ($y=0$), with the experimental data of Fearn *et al.* [7]. (a) Re=26; (b) Re=60; (c) Re =140.

TABLE I. Grid details in the x and z directions and reattachment lengths for the two-dimensional computations with $E=3$ and Re=60.

Grid	N-dx	dx(min,max)	N-dz	dz(min,max)	Reattachment lengths	
A	35	(0.43,22.0)	15	(0.25,0.58)	21.87	7.09
B	50	(0.30,15.0)	21	(0.15,0.43)	21.13	7.23
C	70	(0.20,11.0)	33	(0.10,0.26)	20.89	7.35
D	90	(0.10,9.0)	45	(0.06,0.20)	20.76	7.34
E	110	(0.06,8.0)	57	(0.04,0.18)	20.61	7.34
F	140	(0.04,5.0)	69	(0.02,0.16)	20.38	7.32
G	170	(0.02,4.0)	81	(0.01,0.15)	20.33	7.32

dressed the sidewall induced three-dimensional motion for flows through plane-symmetric sudden expansion at Reynolds number Re=60, and with expansion ratio $E=3$; and for the channel aspect ratio $A>3.5$ flow bifurcations were observed in the step height direction. At this point it is worth mentioning that, in a two-dimensional study for flow through an expansion, Sobey and Drazin [6] reported the existence of multivalued solutions and flow bifurcations. For expansion ratio $E=2$ and Reynolds number Re$\leqslant$11 they observed a unique steady solution that is stable and symmetric. For higher values of the Reynolds number a pitchfork bifurcation occurred and there were two stable asymmetric solutions, and one unstable symmetric solution. As Reynolds number was further increased, they observed four stable asymmetric steady solutions, and three unstable steady solutions, only one of which is symmetric. At Reynolds number close to 100 the flow became unsteady with oscillating reattachment points, and a Hopf bifurcation occurred. Sobey and Drazin [6] also report that the number of stable/unstable and symmetric/asymmetric solutions varied with the value of channel expansion ratio. All these observations motivated us to undertake the present study in three dimensions. In a careful and extensive computational study we observed that, besides the well documented symmetry breaking flow bifurcation in the step height direction (Fig. 4) as observed by the previous investigator, another class of flow bifurcation (Fig. 5) takes place in the spanwise direction. This observed bifurcation phenomenon (Fig. 5) may be viewed as the spanwise separation of the two asymmetric two-dimensional solutions coming together as a symmetric flow at the channel centerline (Fig. 17). To make sure the spanwise bifurcation is real, we conducted several necessary verifications/comparisons.

The remainder of the paper is divided into five sections. The next section describes the mathematical model, which

TABLE II. Grid details in the y direction and numerical details [steady run on Pentium III (800 MHz)] for each three-dimensional computation with $E=3$ and Re=60 at different aspect ratio A.

				Iteration number		CPU time (h)	
A	Grid	N-dy	dy(min,max)	Mode 1	Mode 2	Mode 1	Mode 2
6	C	40	(0.10,0.49)	3500[a]/3500[b]		5.6/5.6	
12	C	40	(0.10,1.22)	3000[a]/3000[b]		4.8/4.8	
18	C	40	(0.10,2.00)	2500[a]/14000[b]		4.0/22.4	
20	C	40	(0.10,2.36)	2500[a]/25000[b]		4.0/40.0	
21	C	40	(0.10,2.51)	2500[a]/65000[b]		4.0/104.0	
22	C	40	(0.10,2.65)	2500[a]	230000[b]	4.0	370.6
24	C	40	(0.10,2.93)	2500[a]	90000[b]	4.0	145.0
27	C	44	(0.10,3.04)	2500[a]	50000[b]	4.5	90.3
30	C	46	(0.10,3.27)	2500[a]	60000[a]	4.7	113.3
36	A	30	(0.25,5.64)	1500[a]	25000[b]	0.4	6.9
36	B	40	(0.15,4.44)	2000[a]	30000[b]	1.5	22.5
36	C	50	(0.10,3.70)	2500[a]	60000[a]	5.2	125.0
36	D	64	(0.07,3.10)	4500[a]	60000[b]	21.3	283.3
36	E	84	(0.04,2.38)	9000[a]	100000[b]	85.0	944.4
36	F	100	(0.02,1.73)	15000[a]	160000[a]	262.5	2800.0
42	C	56	(0.10,3.88)	2500[a]	70000[a]	5.8	161.4
48	C	60	(0.10,4.14)	2500[a]	transient	6.0	933.4

[a]Represents solutions with $u=0$ as the initial guess.

[b]Represents the perturbed model-1 solution, by using reversed solutions with respect to the plane $z=0$ on the left channel or the right channel, as the initial guess.

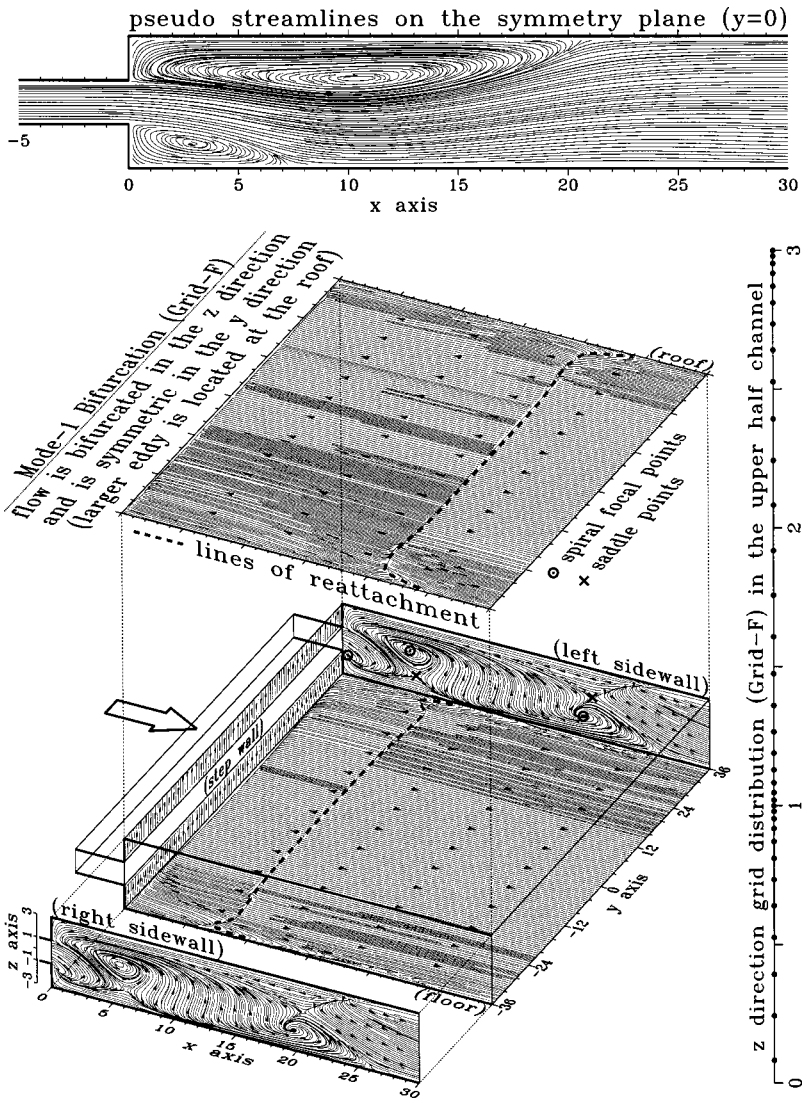

FIG. 4. Three-dimensional illustration of mode-1 surface flow topology and pseudostreamlines on the plane of symmetry $y=0$, for Re $=60$, $A=36$, and $E=3$.

represents the conservation laws for mass and momentum for the incompressible fluid flow. This is followed by presentation of the numerical model for solving Navier-Stokes equations, subject to proper initial and boundary conditions, in three dimensions. Then we present our results. Proper care has been taken while computing the symmetry breaking bifurcation in the spanwise direction. The flow topology extracted from three-dimensional data is also depicted. Finally we make the concluding remarks in Sec. V.

II. MATHEMATICAL MODEL

In this paper we consider the incompressible flow through plane symmetric sudden expansions. The symmetrically configured channel (Fig. 1) is characterized by an expansion ratio E ($\equiv 3$), which is defined as the ratio of the downstream channel height, H, to the upstream channel height, h; and an aspect ratio, A, which is the ratio of the channel span, B, to the upstream channel height, h.

The governing momentum and continuity equations for incompressible flow are cast in the following dimensionless form:

$$\underline{u}_t + \underline{u}\cdot\nabla\underline{u} = -\nabla p + \frac{1}{\mathrm{Re}}\nabla^2\underline{u}, \tag{1}$$

$$\nabla\cdot\underline{u} = 0. \tag{2}$$

The above set of equations accommodates well-posed initial/boundary conditions. This partly explains why the primitive variable formulation has advantages over formulations using the vorticity-based variables [23]. The variables are made dimensionless by using 0.5 times the upstream channel height ($h\equiv 2$), shown schematically in Fig. 1, as the reference length, and 1.5 times the upstream channel mean velocity ($u_{\mathrm{mean}}\equiv\frac{2}{3}$) as the reference velocity, which is prescribed at the channel entry. Based on these referenced quantities, the Reynolds number of the flow is obtained as Re $=(\frac{3}{2}u_{\mathrm{mean}})(\frac{1}{2}h)/\upsilon$, where υ is the kinematic viscosity.

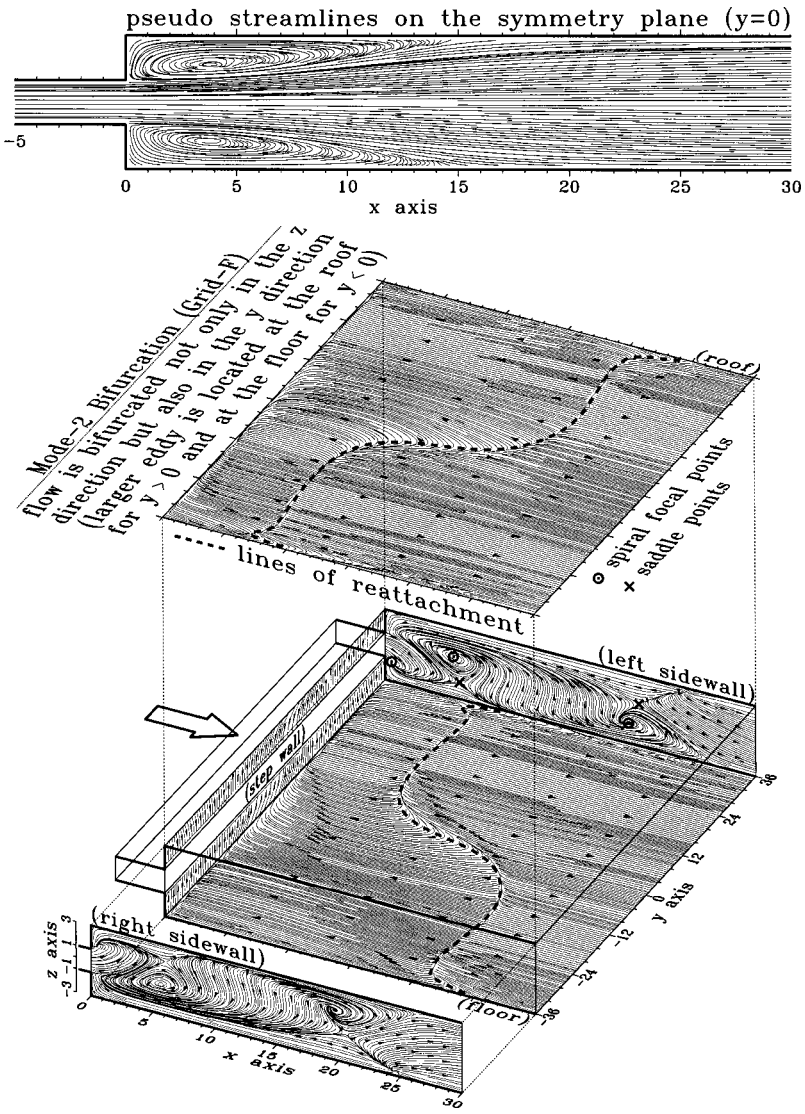

FIG. 5. Three-dimensional illustration of mode-2 surface flow topology and pseudostreamlines on the plane of symmetry $y=0$, for Re $=60$, $A=36$, and $E=3$.

In order to make the above elliptic-parabolic mixed differential equations well posed, we prescribe a uniform velocity $\underline{u}=(\frac{2}{3},0,0)$ at the entry while we prescribe zero gradient conditions at the opposite end of the channel. The inlet length, upstream of the plane of expansion, was chosen as $60h$, while the length of the channel downstream of expansion was taken as $80h$. According to Fearn *et al.* [7], such streamwise upstream/downstream lengths are sufficient for the flow to develop fully. No-slip boundary conditions are prescribed on the confining channel walls. In this paper, we consider mainly the steady state assumption, which has been experimentally confirmed by Fearn *et al.* [7] for flow with $\mathrm{Re}\leqslant 151$. Nevertheless, to obtain additional insights into expanded channel flow, we also conducted transient analyses with flow starting from rest.

III. NUMERICAL MODELING AND VALIDATION

The working equations (1) and (2) were transformed into their discrete counterparts using a finite volume method. In this study, primitive variables were stored on staggered interconnected grids, each of which signified a representative primitive variable [24]. Solutions computed on collocated grids are prone to exhibit pressure wiggles owing to an erroneous treatment of pressure gradient terms. The staggering mesh can effectively overcome the difficulty in this regard. The grid staggering has additional advantage over nonstaggered grids. The reason is that the boundary condition implementation for the equation governing the pressure is unknown. The transient term is approximated by using a fully implicit difference scheme.

Another hurdle in the simulation of fluid flow is the numerical diffusion error. One way to resolve this problem is to apply a QUICK discretization scheme [25] to approximate convection terms in Eq. (1). This scheme is regarded as a refinement of Leonard's original scheme [26] and has been shown to have a stabilizing effect. In addition, the scheme employed here provides third order spatial accuracy. Spatial derivatives other than convective terms in the equations are approximated by means of a second order accurate centered

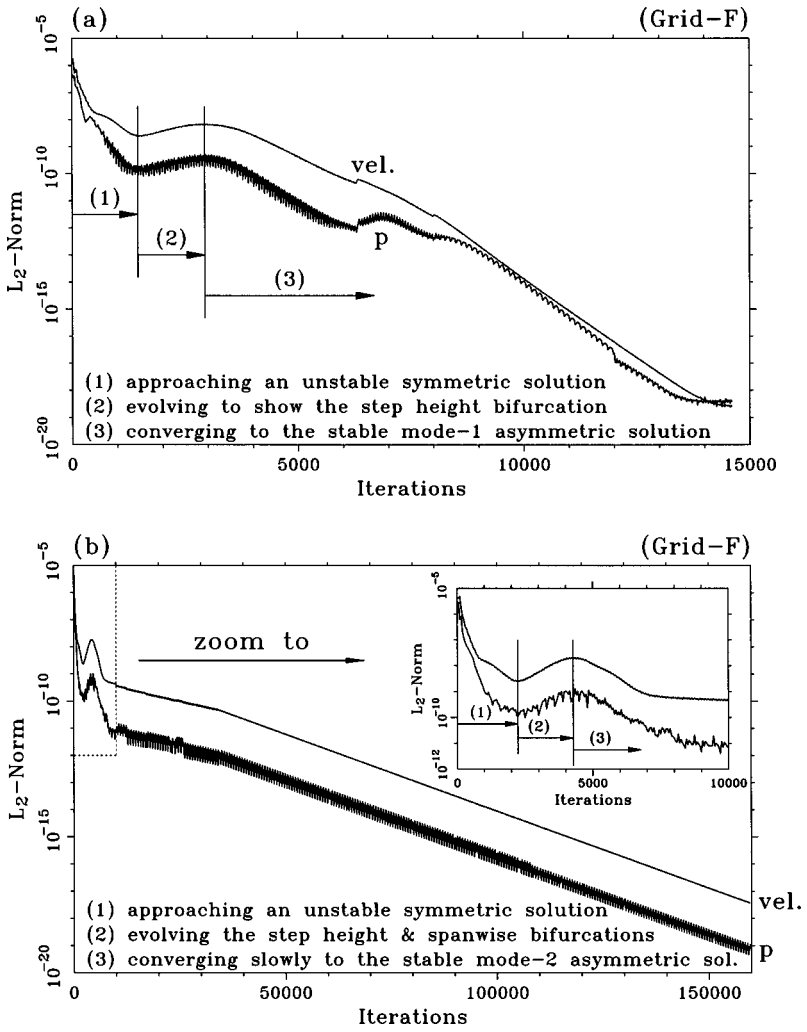

FIG. 6. L_2-error norm convergence history plots for the three-dimensional case with Re $=60$, $A=36$, and $E=3$. (a) Mode-1 bifurcation; (b) mode-2 bifurcation.

scheme. While solving $\underline{u}$ and p from the coupled equations (1) and (2), the absence of pressure term in the continuity equation weakens the discrete system. The segregated approach of Patankar [27] is a well-known method for overcoming such difficulty. In this study, we employ an equation for the pressure difference p' to replace the divergence free continuity equation. This replacement of the working equation enables us to apply a semi-implicit iterative algorithm, thus reducing the disk storage requirement. In this paper, we applied a solution algorithm, which is similar to SIMPLE-C [28], to solve three momentum equations for $\underline{u}$ and one Poisson equation for the p' in a "predict and correct" cyclic process.

In all the cases investigated, the iterative calculation of primitive variables was terminated, subject to the L_2-residual norm criteria ($\leqslant 10^{-18}$) set for pressure and velocity. In addition, we ensure that mass flux q_i at each streamwise cross section satisfy $|q_i-q_0|/q_0<10^{-10}$, where q_0 is the specified mass flux of the entry flow. The details of the solution algorithm implementation and its analytical validation are presented in our previous work [22,29]. For the sake of comparison of the present result with the experimental measurements of Fearn *et al.* [7], we conducted computations for the flow, and an excellent agreement was achieved (Figs. 2 and Fig. 3). To ensure that the computed solutions represent the real flow physics, we conducted a series of grid independence tests, the details are listed in Table I. The grids mainly employed in this study are grid *C* and grid *F*, which ensure that the size of the eddy captured remained independent of mesh size. To extract a realistic flow feature, we performed calculations in the full domain of the physical problem schematically shown in Fig. 1. Nonuniform grids were used, with finer grids clustered near the step and in the vicinity of nonslip walls. Six grids of different resolutions were considered and shown in detail in Table I and Table II, including the CPU used on a Pentium III (800 Mhz).

IV. RESULT AND DISCUSSION

Discussion of the results is organized as follows. We start with presenting the flow topology to give a global picture of the three-dimensional flow development in the expanded channel. We then assert that a symmetry breaking bifurcation of the flow takes place at Re$=60$ in a channel with $E=3$. In

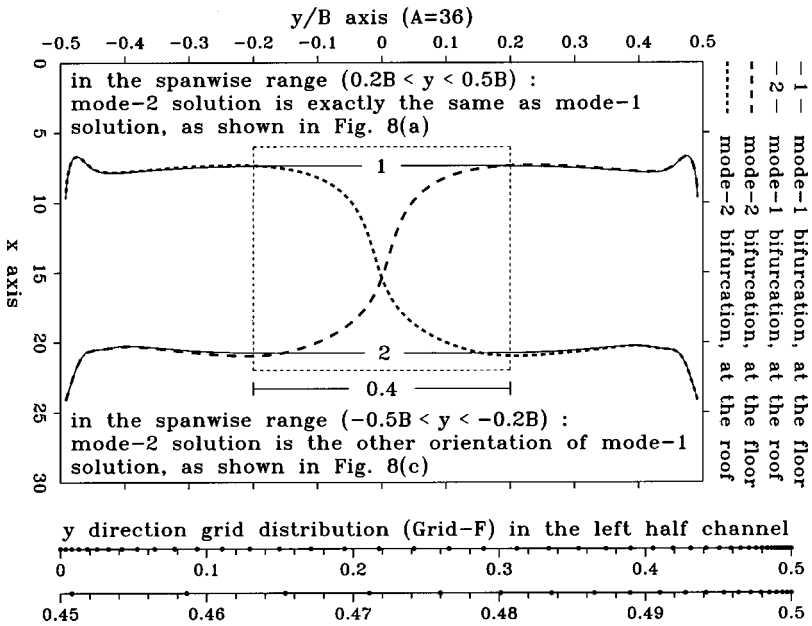

FIG. 7. Lines of reattachment on the channel roof and floor for two bifurcation modes of asymmetric solutions. The flow condition used is Re $=60$, $A=36$, and $E=3$.

addition to our previous study [22], we found that the flow bifurcation occurs, not only in the step height direction, but it bifurcates also in the spanwise direction. Extensive numerical verifications have been made to ascertain that the observed spanwise symmetry breaking solution is not of numerical origin. To this end, we conduct a lengthy time-accurate transient calculation. Having confirmed the existence of two modes of symmetry breaking flow in the suddenly expanded channel, it is natural to provide a critical value of the aspect ratio, below which no flow asymmetry may be expected to exist in the spanwise direction. Furthermore, we have also conducted a parametric study on variations of Re and E to show and establish the fact that the symmetry breaking bifurcation in the spanwise direction is a

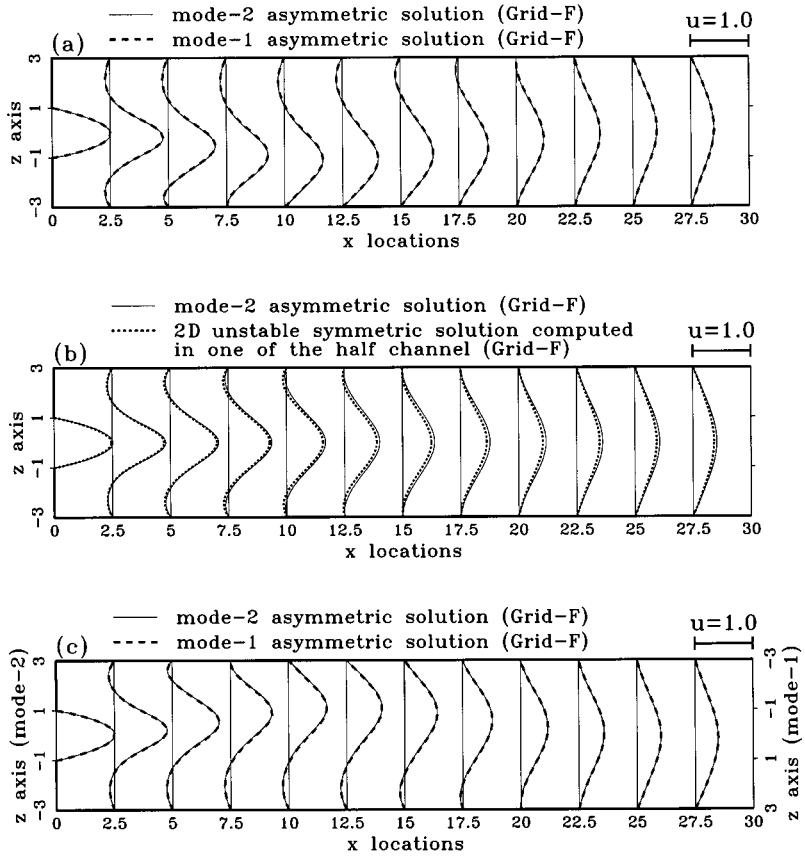

FIG. 8. Plots of the streamwise velocity (u) profiles along the spanwise direction, showing two bifurcation modes of solutions computed at Re$=60$, $A=36$, and $E=3$. (a) $y=0.3B$; (b) $y=0$; (c) $y=-0.3B$.

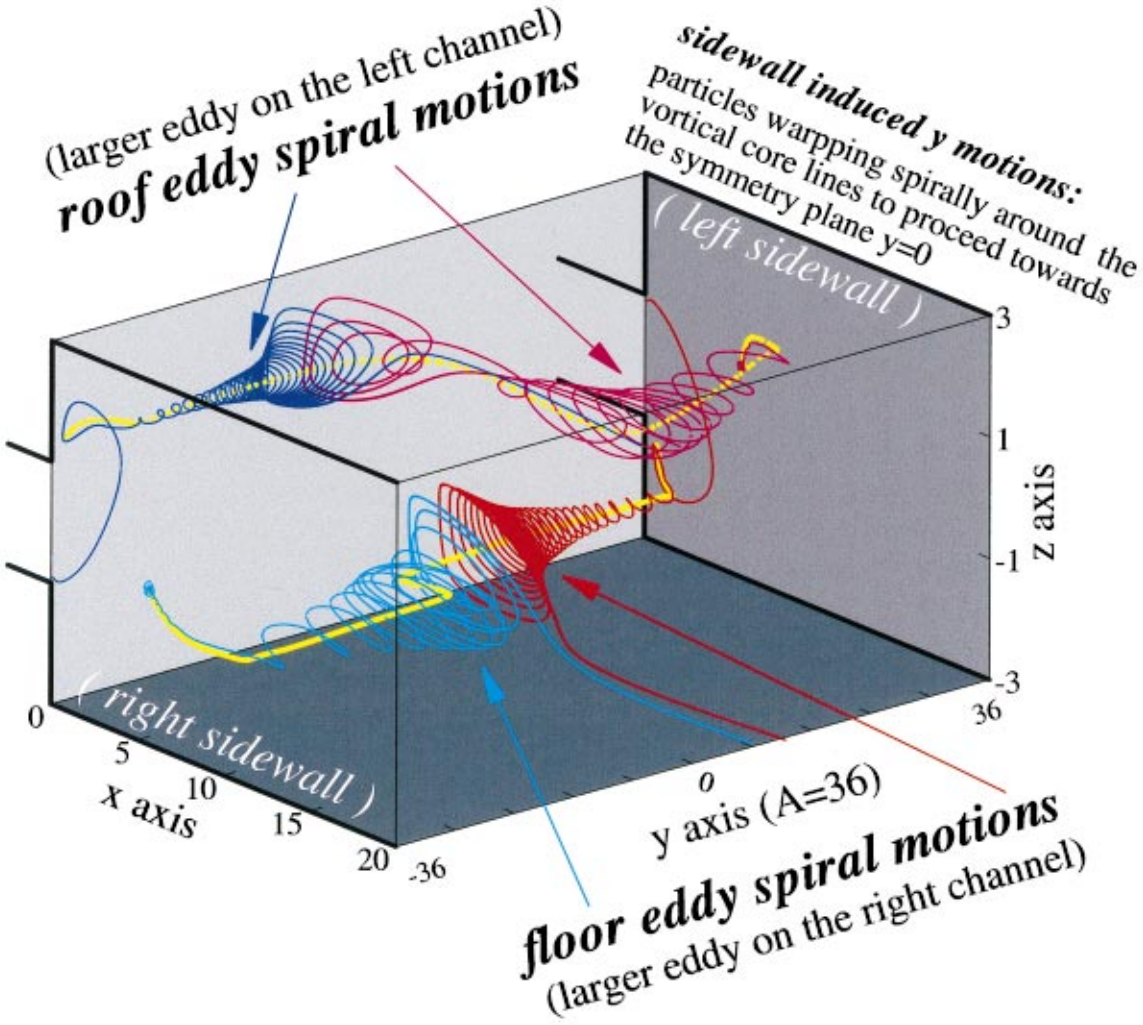

FIG. 9. (Color) Illustration of spiraling particles warping the vortical core lines in the mode-2 bifurcated flows for Re=60 and with $A=36$ and $E=3$.

general phenomenon of the plane symmetric sudden expansion flows.

A. Flow topology

To effectively obtain a profound understanding of the three-dimensional character of the flow structure, one may resort to the topology of limiting streamlines [30] or skin friction lines [31] in order to extract meaningful flow physics from an enormous amount of computed data. In this paper, limiting streamlines, which are by definition streamlines passing very close to the solid wall, are chosen to depict the flow structure. The limiting streamlines are known to diverge from lines of reattachment [32], and the converse of lines of reattachment is lines of separation. While approaching the lines of separation, neighboring streamlines tend to converge. By marking use of the kinematic nature of limiting streamlines, we classify singular nodes, foci, and saddles. These topological singular points supplemented with lines of separation and reattachment, as plotted in Fig. 4 for the step height bifurcation flow at Re=60 in a channel with $E=3$ and $A=36$, can depict the three-dimensional flow structure, and thus provide us with additional flow details as illustrated in our previous paper [22].

Symmetry breaking flows bifurcated in the step height direction, as shown in Fig. 4, can have two orientations. As the primary stream bends towards the channel roof, a large eddy is seen on the channel floor. On the other hand, a large eddy is seen on the channel roof, provided the primary stream is bent towards the channel floor. In the present study, we report that the two orientations of the step height symmetry breaking bifurcation flow can coexist in the channel as shown in Fig. 1.

B. Two stable modes of symmetry breaking bifurcation

Results obtained from the present study, for flow with Re=60 in a channel with $E=3$ and $A=36$, show the presence of two possible modes of pitchfork bifurcation. One is shown in Fig. 4, and the other, which was not seen in our previous study [22], is depicted in Fig. 5. In the following discussion of the results, we refer to the solution that is

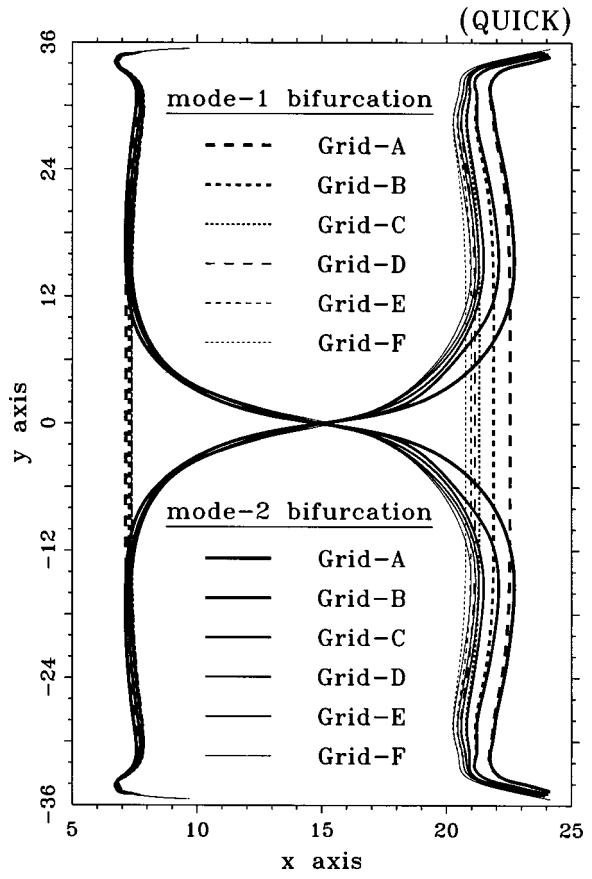

FIG. 10. Comparison of the lines of reattachment, for mode-1 and mode-2 bifurcations, representing the grid independence. All solutions were obtained by using the QUICK scheme at Re=60 and with $A=36$ and $E=3$.

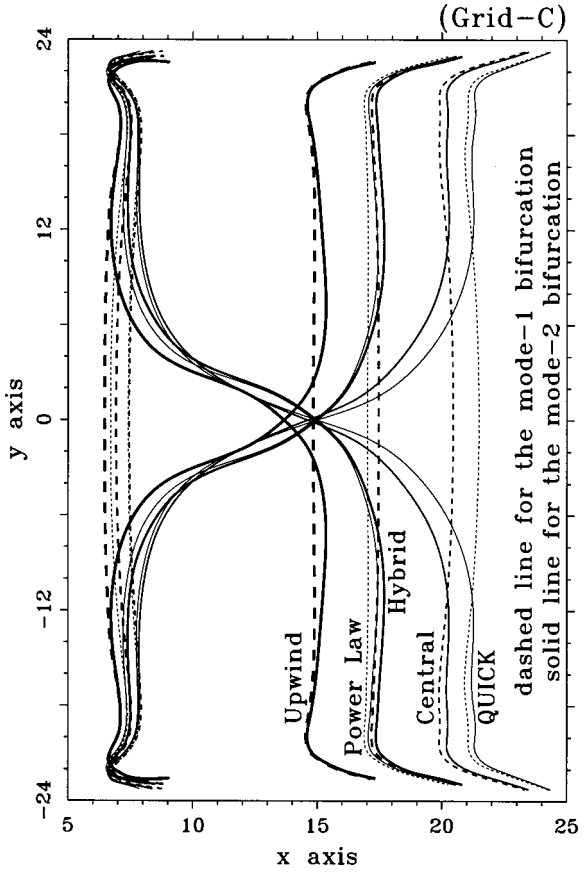

FIG. 11. Comparison of the lines of reattachment, for mode-1 and mode-2 bifurcations, representing the scheme independence. All solutions were obtained on grid C at Re=60 and with $A=24$ and $E=3$.

asymmetric in the step height (z) direction but is symmetric in the spanwise (y) direction as the mode-1 solution (Fig. 4). The mode-2 solution is defined as being asymmetric in both y and z directions (Fig. 5).

As the flow evolved to exhibit mode-1 bifurcation feature as shown in Fig. 4, the lines of reattachment on the channel roof and floor remained relatively invariant in the spanwise direction, with the exception in regions near the two sidewalls. Unlike the mode-1 bifurcated flow, considerable discrepancy in the flow nature between the two halves of the channel with $y<0$ (the right half of the channel) and $y>0$ (the left half of the channel) was observed in the mode-2 bifurcation. The lines of reattachment on channel roof and floor for the flow evolving into the mode-2 symmetry-breaking pattern is shown in Fig. 5. In mode-2 bifurcation the eddy size at the roof became larger than that at the channel floor in the left-half channel ($y>0$), while the opposite trend of eddy size is found in other half channel ($y<0$) for the case with $A=36$. On the plane of symmetry $y=0$ as shown in Fig. 5, the reattachment lengths at the channel roof and floor are identical. Hence on the symmetry plane $y=0$, the mode-2 bifurcated flow is symmetric in the step height direction. Also noteworthy is the flow topology on the left sidewall, whose orientation is antisymmetric to that on the right sidewall as shown in Fig. 5.

To show that y and z direction symmetry breaking flows are indeed stable, we provide the history of convergence behaviors [Fig. 6(a)] for flows evolving via mode-1 bifurcation, and via mode-2 bifurcation [Fig. 6(b)]. For both cases, twelve orders of magnitude of the L_2-error norms have been reduced for $\underline{u}$ and p. Besides iteration residuals set as low as 10^{-18}, the present calculation requires the relative difference of mass fluxes between inlet plane and other arbitrary chosen cross flow planes be less than 10^{-13}. It may be noted that the error reduction rate is much slower while approaching the convergent mode-2 solution. To be more precise, it takes roughly ten times iteration number to obtain a convergent mode-2 asymmetric solution than that needed to obtain the convergent mode-1 asymmetric solution. Moreover, computing mode-2 bifurcation is rather a difficult task (we shall explain this behavior in another section). As a further check, whether the two modes of bifurcated flows are numerically stable, we perturbed both flows randomly by altering their values by an amount of 10 to 20 percentages and continued the calculations. The solutions obtained under stringent convergence criteria mentioned earlier reproduced the solutions, as shown schematically in Figs. 4 and 5, for mode-1 and mode-2 bifurcation solutions, respectively. It suffices to assert that more than one symmetry-breaking bifurcation is possible for the channel flow under investigation.

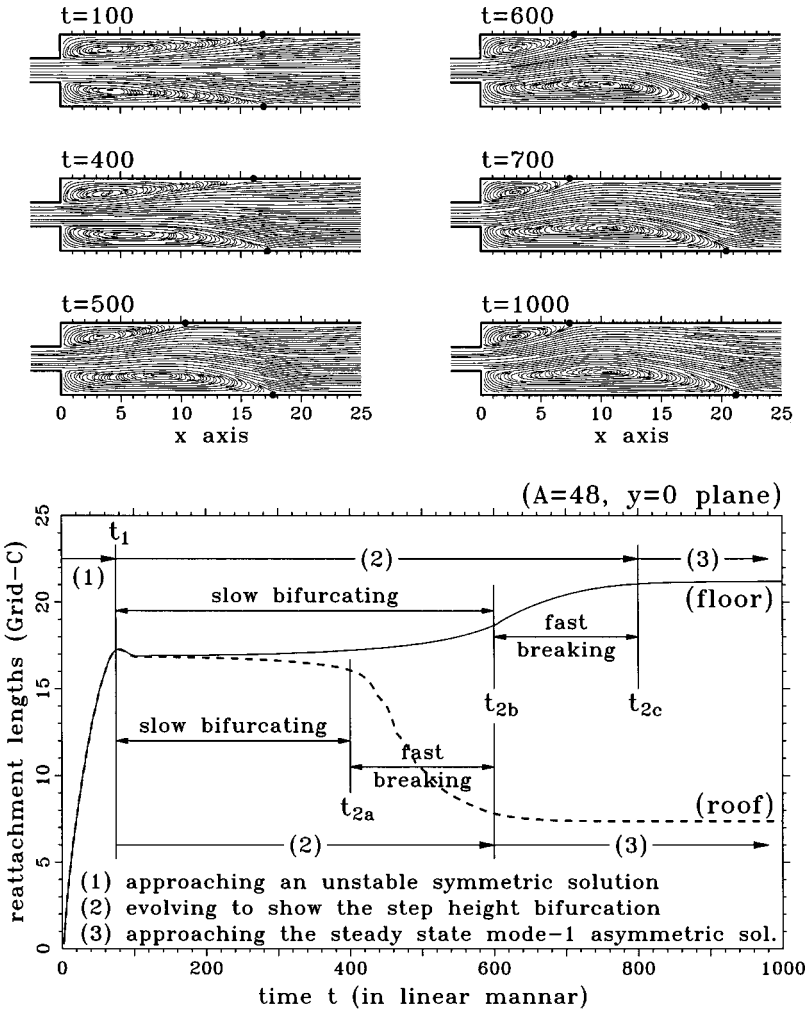

FIG. 12. The mode-1 time evolving reattachment lengths on the channel roof and floor of the plane of symmetry $y=0$. The flow condition used is Re=60, $A=48$, and $E=3$.

C. Bifurcation natures

To provide a clear picture indicating the difference in topologies in two bifurcation modes in the channel flow, in Fig. 7 we plot the spanwise distributions of reattachment lengths on the channel floor and the channel roof. It is interesting to observe that the reattachment lines in mode-2 bifurcation are not only confined between the lines of reattachment (at channel roof and channel floor) for mode-1 bifurcation, but they also conserve the streamwise extension. In the spanwise range $0.2B \leqslant y \leqslant 0.5B$ (the left side), the mode-2 bifurcation is exactly the same as the mode-1 bifurcation. Thus there exists a good agreement between the streamwise velocity profiles on the plane $y=0.3B$ for two modes of solution plotted in Fig. 8(a). Also, in the opposite spanwise range $-0.5B \leqslant y \leqslant -0.2B$ (the right side), the mode-2 bifurcation is just the same as the other orientation of the mode-1 bifurcation. Thus, the streamwise velocity profiles of two modes, on the planes $y=-0.3B$ shown in Fig. 8(c) are antisymmetric with respect to the plane $z=0$. In the core region (Fig. 7), highlighted in the window block with spanwise length $0.4B$, mode-2 flow tends to become symmetric while remaining bounded by the different orientations of step height bifurcations on the left and right sides. The profile of the reattachment length on the channel floor is antisymmetric to that on the channel roof in spanwise core region $|y| \leqslant 0.2B$ $(=7.2h)$ for the mode-2 bifurcation flows. These antisymmetric reattachment line profiles, which evolved via mode-2 bifurcation, have a z symmetry profile, which is nearly the same as the unstable solution computed from the two-dimensional analysis, at the symmetry plane $y=0$, and is shown in Fig. 8(b). It shows that the mode-2 asymmetric solutions are the different orientations of mode-1 asymmetric solutions on the left and right sides of the channel, respectively, with a symmetric solution on the symmetry plane $y=0$. That means there coexist two stable solutions and an unstable solution of two-dimensional flow in the suddenly expanded channel.

One way of exhibiting the three-dimensional flow nature is to trace the path of particles originating from the spiral focal points on the sidewalls. The sidewall boundary layer imposes shear resistance on the primary motion of fluid particles immediately behind the step. This results in a spanwise pressure gradient and, in turn, an increasingly large spanwise velocity component. This non zero spanwise velocity causes particles, as shown in Fig. 9 indicating the mode-2 flow bifurcation, to wrap spirally around the vortical core while proceeding towards the symmetry plane $y=0$.

Prior to turning to the next section, it is important to establish that the mode-2 bifurcation is physically realistic for the channel flow with Re=60 and $E=3$. For this reason, we

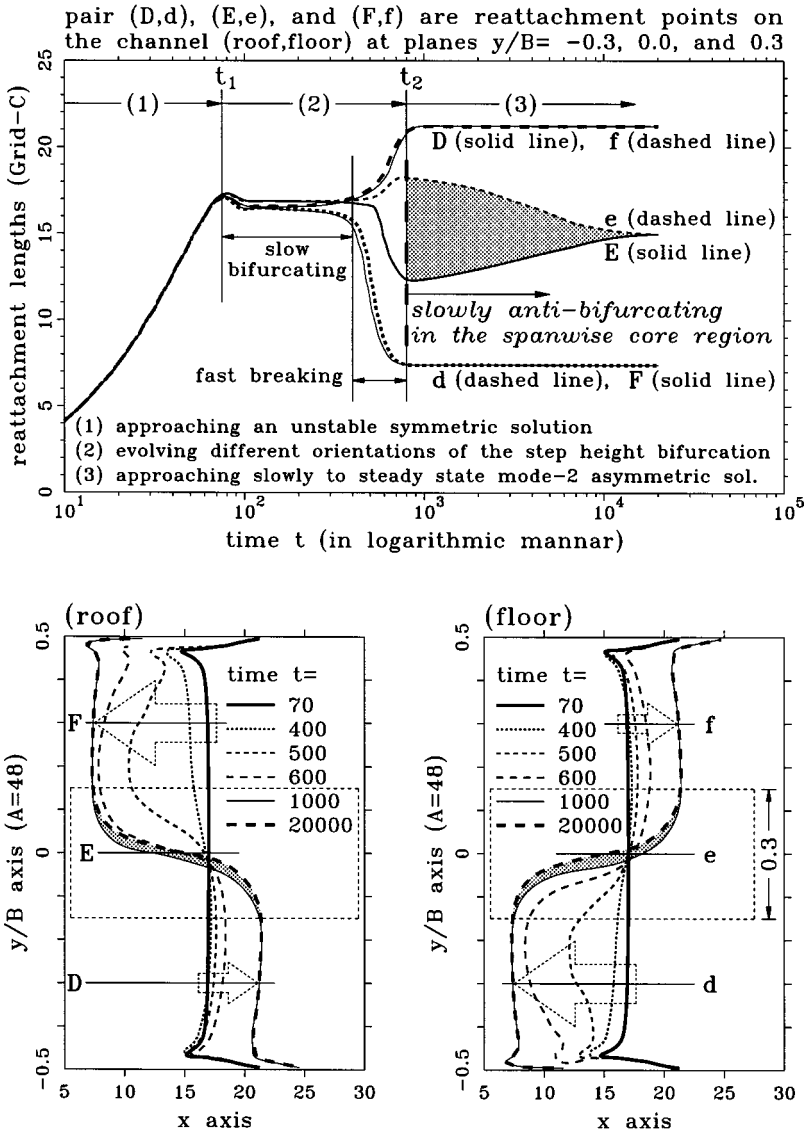

FIG. 13. The mode-2 time evolving reattachment lengths on the channel roof and floor at planes $y=-0.3B$, 0, and $0.3B$. The flow condition used is Re=60, $A=48$, and $E=3$.

once again present evidence that shows the predicted two modes of bifurcation solutions are independent of grids used and the discretization schemes adopted. To demonstrate that our predicted symmetry breaking phenomena are independent of the grid used, we conducted calculations on six grids of different mesh resolutions shown in Table II to solve the problem for $A=36$, and the computed modes of bifurcation are shown in Fig. 10. We also employed five different convection discretization schemes, of first order to third order accuracy, respectively, to solve the problem for $A=24$ on grid *C*. Figure 11 shows that the physical behavior remains the same and has no dependence on the schemes chosen. The above grid independent and scheme independent tests certify that the presently predicted two modes of bifurcation phenomena are real and physical, and not generated due to any computational inadequacy.

D. Transient analysis

To study the temporal evolution of the two modes of bifurcation for the plane symmetric sudden expansion flows, we conducted also the time consuming three-dimensional transient calculation at Re=60. Given the initially quiescent flow condition, we solved the time dependent elliptic-parabolic Navier-Stokes equations in the channel with $E=3$ and $A=48$.

When the flow evolves to form the symmetry breaking mode-1 bifurcation in the step height direction, the nature of bifurcation is invariant along the spanwise direction. In Fig. 12 we plot the mode-1 time varying reattachment lengths on the channel roof/floor on the plane of symmetry $y=0$. The flow retains symmetry in the step height direction during $0<t<t_1$ of the flow development. During the period, the eddy sizes on the channel roof/floor remained equal while getting increased linearly to reach a local maximum value; that is a two-dimensional unstable symmetric solution. Since this flow cannot be stably retained, the flow starts exhibiting symmetry breaking bifurcation at $t=t_1$. Afterwards, the bifurcation period is categorized into two stages, a slow bifurcating period and a fast breaking period. In the process, the lengths of reattachment varied and the floor eddy size increased by 25% and the roof eddy size decreased by about 55% of the symmetric value at $t=t_1$. By $t\sim10^3$, the bifur-

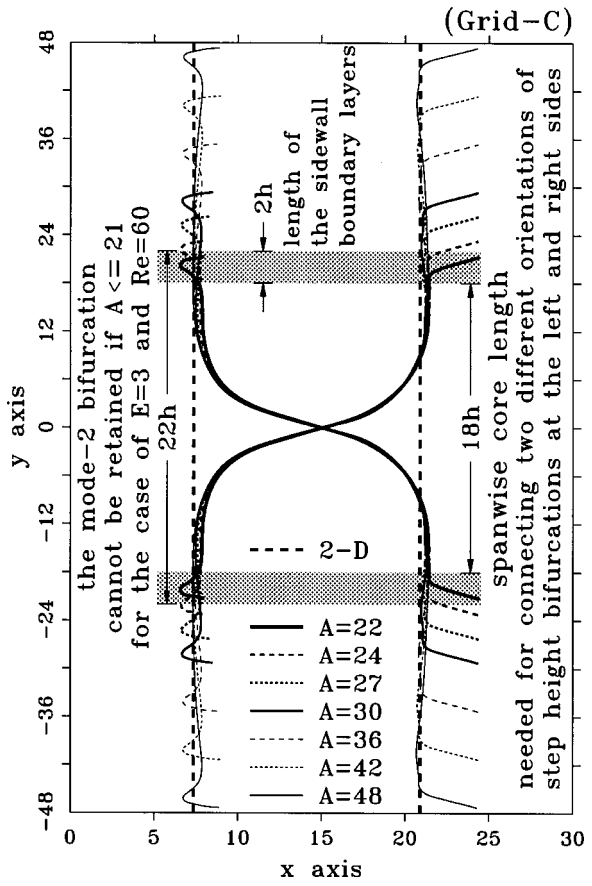

FIG. 14. Comparison of lines of reattachment of mode-2 bifurcation on the channel roof and floor, at Re=60 and $E=3$, for different aspect ratios $A=22$, 24, 27, 30, 36, 42, and 48.

cated flow has reached its steady state. It may be noted from Fig. 4 that the mode-1 solution has another orientation. For $A=36$, Fig. 4 shows the eddy size on the floor is smaller than the eddy size on the channel roof, and therefore exhibits a reverse orientation of mode-1 bifurcation compared to the case with $A=48$, as shown in Fig. 12.

The transient behavior of the mode-2 symmetry breaking bifurcation is shown in Fig. 13. The reattachment lengths on the planes $y=-0.3B$, 0, and $0.3B$, increased/decreased all the way up to their asymptotic values. For purposes of completeness, we also plot the distribution of lines of reattachment on the channel roof/floor at $t=70$, 400, 500, 600, 1000, and 20 000 in the same figure. Similar to mode-1 flow bifurcation, up to time $t\sim t_1$ the flow shows the unstable symmetric structure, which cannot be stably retained. Afterwards, flow gradually loses stability and evolves eventually to a bifurcation first through a slowly evolving process and then at a much faster process in a relatively short time period. During $t_1<t<t_2$ the formation of step height symmetry breaking bifurcation, the mode-1 flow (Fig. 12) remained symmetric (i.e., with unanimous orientation) along the spanwise direction, but maintained opposite orientation in the left and the right channel for mode-2 flow (Fig. 13). Figure 13 also shows the evolution of spanwise bifurcation via step height bifurcation, and the formation of large eddy at the right channel roof and left channel floor. The converse phenomenon was observed in Fig. 5. To be explicit, for $A=36$ (Fig. 5) the eddy size at the roof became smaller than the eddy size at the channel floor in the right channel, and the opposite trend of the eddy size is observed in the left channel. This means the mode-2 bifurcation, similar to the mode-1 bifurcation, can have two orientations. The evolving process of spanwise symmetry breaking via step height bifurcation, as shown in Fig. 13 for the case with $A=48$, can be clearly observed from the movement of the lines of reattachment on the roof/floor during the period $t=70-1000$. Therefore, the mode-2 bifurcation, where flow bifurcates in spanwise direction, evolves from different orientations of step height bifurcations at the left and right sides of the channel separately. At a time roughly equal to 10^3, mode-2 flow (Fig. 13) has almost reached the steady state solution, with the exception in the spanwise core region $|y|\leqslant 0.15B$ $(=7.2h)$ where flow still undergoes a fairly slowly evolving process in an antisymmetric sense. The slow convergence of points "*e*" and "*E*" shown in Fig. 13 may suggest that there is another time scale related to spanwise lengths and velocities. The spanwise core flows during $t=10^3\sim 10^4$ complete the whole evolution process (Fig. 13), and the flow became symmetric in the step height direction on the plane of symmetry $y=0$.

The much slower convergence schematic in Fig. 6(b) and the slow temporal evolution shown in Fig. 13 reveals that mode-2 flow is difficult to obtain, compared to the mode-1 flow. One physically meaningful reason for such difficulty is the coexistence of symmetric solution on $y=0$ and the antisymmetric solutions for $y>0$ and $y<0$. The symmetric flow on the symmetry plane $y=0$ is unstable in the sense that such a symmetric solution is impossible to obtain from the two-dimensional analysis.

E. Critical aspect ratio for spanwise bifurcation

The flow features with aspect ratios $A=36$ and $A=48$, presented in Fig. 7 and Fig. 13, respectively, reveal that the appearance of mode-2 bifurcation requires long enough spanwise core length for evolving from two different orientations of step height bifurcation. Therefore it will exist at a critical aspect ratio A_c, and for $A>A_c$ we can obtain symmetry breaking bifurcation in the spanwise direction. In the present study, we varied the aspect ratio in the range of $6\leqslant A\leqslant 48$ and examined carefully the computed results in the spanwise direction for $E=3$ and Re=60.

It has been found that the two modes of symmetry breaking bifurcation with initial guess $\underline{u}=0$ can be obtained provided that aspect ratio $A\geqslant 30$. For aspect ratios $A<30$, only mode-1 symmetry breaking bifurcation takes place (with initial guess $\underline{u}=0$), but not the mode-2 solution. Upon perturbation of the computed mode-1 solution, by using the reversed solutions with respect to the plane $z=0$ on the left or the right channel, and using them as the initial guess and proceeding the calculation, the flow evolves into the stable mode-2 bifurcation for aspect ratios $A=27$, 24, and 22, whereas they go back to their mode-1 form eventually for lower values of the aspect ratios $A=21$, 20, 18, 12, and 6. Based on the calculation details in Table II, we found that the

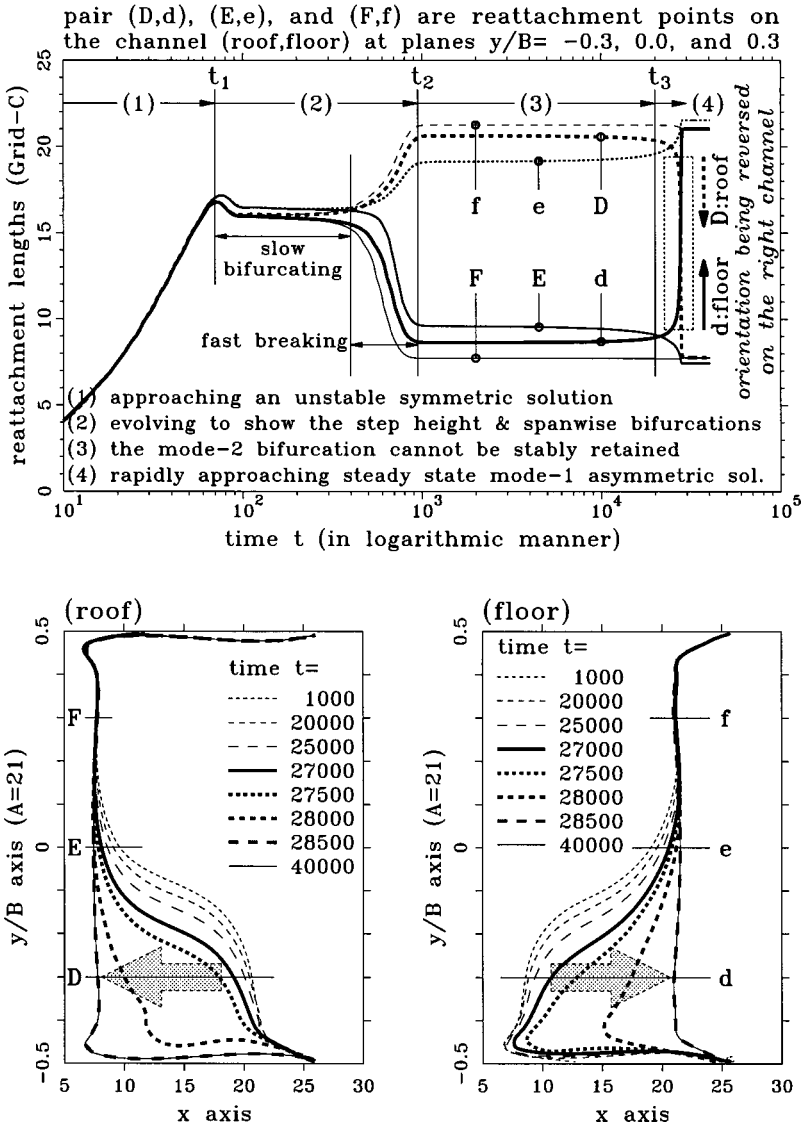

FIG. 15. Time evolving reattachment lengths on the channel roof and floor, on planes $y=-0.3B$, 0, and $0.3B$, showing the spanwise bifurcation may not be retained for $A=21$. The flow condition used is Re=60 and $E=3$.

critical value of the aspect ratio is $A_c=21$ for mode-2 bifurcation to occur in a channel with $E=3$ and Reynolds number Re=60. In the experiment Fearn *et al.* [7] considered the case with aspect ratio 24 but observed no spanwise symmetry breaking bifurcation for Reynolds numbers up to 140. For $A=24$ being located near the critical region $A_c=21$, the appearance of the mode-2 bifurcation may require a suitable perturbation of the flow. Moreover, we found that the critical aspect ratio for the occurrence of the mode-2 bifurcation is also dependent on flow Reynolds numbers. Our computation results show that no mode-2 bifurcation can be stably retained for cases with $A=24$ and 27, and Re=140. This partially explains why Fearn *et al.* [7] missed the mode-2 bifurcation.

For seven different investigated cases with $A>A_c$, we plot in Fig. 14 the lines of reattachment on the channel roof and floor for flows evolving to mode-2 bifurcated solution. It is surprising to observe that the lines of reattachment fall into the same line and have no functional dependence on A in the spanwise core region of $|y|\leqslant 9h$. To further justify the stability of the mode-2 flow for the critical aspect ratio 21 and Re=60 in a channel with $E=3$, we conducted the transient calculations starting with $\underline{u}(\underline{x},t=0)=0$, and then perturbed the process (as mentioned above) at $t=10$ and proceeded the computation. We plot in Fig. 15 the computed reattachment length on the channel roof and floor against time on the planes $y=-0.3B$, 0, and $0.3B$. This bifurcation diagram also shows the same evolving process as observed in the channel with $A=48$ (Fig. 13). The flow evolves first to produce the symmetric solution, which cannot be stably retained. This is followed by a slowly and then a rapidly evolving processes to produce the mode-2 symmetry breaking bifurcation. The mode-2 bifurcated flow did not reach a steady state until $t\sim 2\times 10^4$. During the time period $t=27200-28200$ the flow quickly approached towards the mode-1 solution. In the process, the right channel flow reversed its symmetry breaking orientation, and became the same as the left channel flow.

F. Parametric study on Reynolds number and expansion ratio

It has been observed that the two modes of symmetry breaking flows can be stably retained for the flow at Rey-

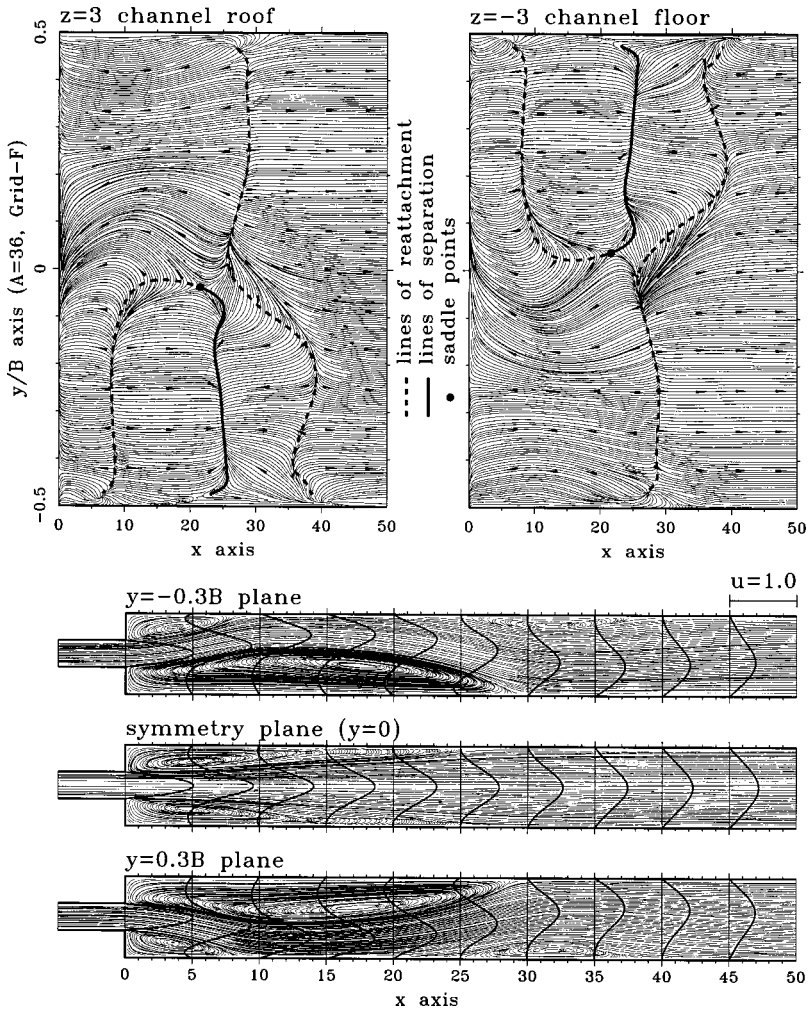

FIG. 16. Limiting streamlines on the channel roof/floor and pseudostreamlines on planes $y=-0.3B$, 0, and $0.3B$ showing the mode-2 bifurcation. The flow condition used is Re=100, $A=36$, and $E=3$.

nolds number Re=60 in the channel with expansion ratio $E=3$. To confirm that such a multiple bifurcation is not a particular case but a general phenomenon, we vary Reynolds number Re and expansion ratio E subsequently to study their effects on the bifurcation nature of the flow in the suddenly expanded channel.

We carried out calculations on grid F in a channel with $A=36$ and $E=3$ at three different Reynolds numbers Re =80, 100, and 120. The results show that mode-1 and mode-2 solutions are possible to obtain at these Reynolds numbers and can both reach their respective steady state solutions. We plot in Fig. 16 the roof/floor flow topologies and pseudostreamlines on planes $y=-0.3B$, 0, and $0.3B$ for mode-2 bifurcation at Re=100. One noteworthy feature of this channel flow is the formation of a third eddy in the spanwise y planes. What is more important to note from the developed flow at this higher Reynolds number is the complexity of the flow topology (Fig. 16). On the channel roof and floor, limiting streamlines manifest themselves by showing additional lines of separation, which connect lines of reattachment at the saddle point. The complexity in flow topology shows that three-dimensional flow behavior prevails in the channel. Such a flow pattern, in the spanwise core region, is not due to the sidewall effect, but is rather produced by internal affairs. The flow topology on the roof and the floor as observed from Fig. 16 show that the notion of the pitchfork takes on a whole different meaning here.

According to the two-dimensional result of Drikakis [14], the critical Reynolds numbers, above which the flow starts bifurcating, are 108 and 26.5 for $E=2$ and $E=4$, respectively. Just to have a feeling in three dimensions, we carried out calculations on grid C in a channel with $A=36$ and $(E,\mathrm{Re})=(2,125)$ and (4, 40). In addition to the two-dimensionally predicted mode-1 bifurcation in the step height direction, mode-2 solutions are also observed, and are graphically shown in Fig. 17.

V. CONCLUDING REMARKS

In the present paper, we have explored the existence of a second mode of bifurcation in a plane-symmetric channel with sudden expansion. Consideration has been given to establish the presence of Coanda phenomenon in both the step height and spanwise directions. Through this detailed numerical study, it is found that two modes of symmetry breaking flow can be stably retained in the geometrically symmet-

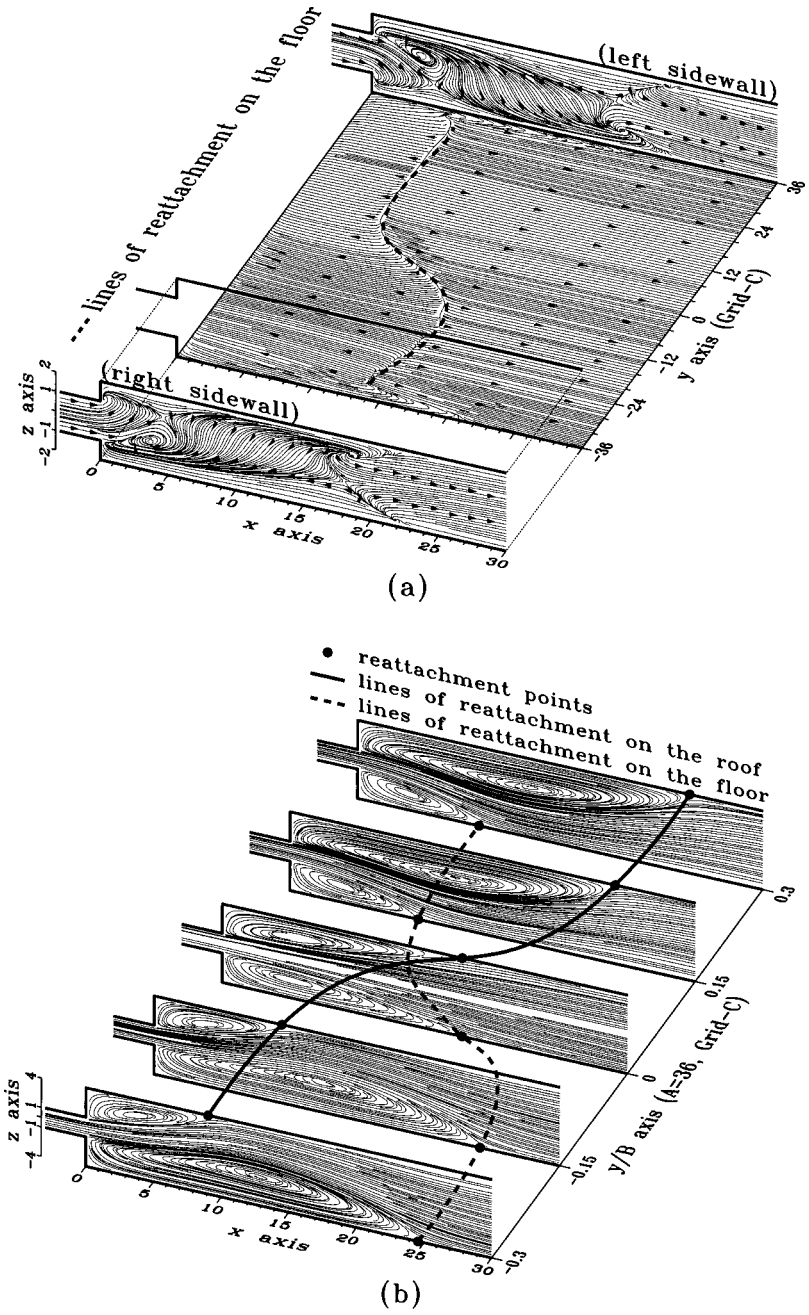

FIG. 17. Three-dimensional plot of the surface flow topology showing the mode-2 bifurcation. (a) Re=125, $A=36$, and $E=2$; (b) Re =40, $A=36$, and $E=4$.

ric channel. The step height bifurcation (mode-1), which exists in two-dimensional flow, can also have a spanwise (mode-2) counterpart. Moreover, both mode-1 and mode-2 bifurcations can have two orientations. Reattachment lines for the mode-2 flow have a streamwise extension, which connects and coincides with the two different orientations of mode-1 flow on the left and right sides. Results indicate that two stable asymmetric solutions and one unstable symmetric solution are coexisting in the mode-2 flow. Besides the steady state analysis, transient behavior of the flow has been studied. Compared to mode-1 bifurcation, the mode-2 bifurcation is more difficult to obtain, due to the unstable flow symmetry at the spanwise symmetry plane. For channel flows with aspect ratio less than the critical value, i.e., $A \leqslant A_c$, the originally occurring mode-2 bifurcation cannot be stably retained and will evolve into mode-1 bifurcation eventually. Parametric studies on Reynolds numbers and channel expansion ratios were also conducted to improve our understanding about the three-dimensional nature of the suddenly expanded channel flows.

ACKNOWLEDGMENTS

Support for this research provided by the National Science Council of the Republic of China under Grants No. NSC87-2213-E-002-002 and No. NSC88-2611-E-001-001 is gratefully acknowledged.

[1] E. O. Macagno and T. K. Hung, J. Fluid Mech. **28**, 43 (1967).
[2] F. Durst, A. Melling, and J. H. Whitelaw, J. Fluid Mech. **64**, 111 (1974).
[3] W. Cherdron, F. Durst, and J. H. Whitelaw, J. Fluid Mech. **84**, 13 (1978).
[4] I. J. Sobey, J. Fluid Mech. **151**, 395 (1985).
[5] D. J. Latornell and A. Pollard, Phys. Fluids **29**, 2828 (1986).
[6] I. J. Sobey and P. G. Drazin, J. Fluid Mech. **171**, 263 (1986).
[7] R. M. Fearn, T. Mullin, and K. A. Cliffe, J. Fluid Mech. **211**, 595 (1990).
[8] F. Durst, J. C. F. Pereira, and C. Tropea, J. Fluid Mech. **248**, 567 (1993).
[9] R. Wille and H. Fernholz, J. Fluid Mech. **23**, 801 (1965).
[10] P. S. Scott and F. A. Mirza, Comput. Fluids **14**, 423 (1986).
[11] M. Shapira and D. Degani, Comput. Fluids **18**, 239 (1990).
[12] E. A. Foumeny, D. B. Ingham, and A. J. Walker, Comput. Fluids **25**, 335 (1996).
[13] J. Mizushima, H. Okamoto, and H. Yamaguchi, Phys. Fluids **8**, 2933 (1996).
[14] D. Drikakis, Phys. Fluids **9**, 76 (1997).
[15] N. Alleborn, K. Nandakumar, H. Raszillier, and F. Durst, J. Fluid Mech. **330**, 169 (1997).
[16] T. Hawa and Z. Rusak, Phys. Fluids **12**, 2257 (2000).
[17] T. Hawa and Z. Rusak, J. Fluid Mech. **436**, 283 (2001).
[18] D. Drikakis and A. Spentzos, in *Parallel Computational Fluid Dynamics: Recent Developments and Advances Using Parallel Computers*, edited by D. R. Emerson *et al.* (Elsevier Science B.V., Amsterdam, 1998), p. 317.
[19] A. Baloch, P. Townsend, and M. F. Webster, Comput. Fluids **24**, 863 (1995).
[20] E. Schreck and M. Schäfer, Comput. Fluids **29**, 583 (2000).
[21] F. Battaglia, S. J. Tavener, A. K. Kulkarni, and C. L. Merkle, AIAA J. **35**, 99 (1997).
[22] T. P. Chiang, Tony W. H. Sheu, and S. K. Wang, Comput. Fluids **29**, 467 (2000).
[23] O. A. Ladyzhenskaya, *Mathematical Problems in the Dynamics of a Viscous Incompressible Flow* (Gordon & Breach, New York, 1963).
[24] F. H. Harlow and J. E. Welch, Phys. Fluids **8**, 2182 (1965).
[25] T. P. Chiang, Robert R. Hwang, and W. H. Sheu, Int. J. Numer. Methods Fluids **23**, 325 (1996).
[26] B. P. Leonard, Comput. Methods Appl. Mech. Eng. **19**, 59 (1979).
[27] S. V. Patankar, *Numerical Heat Transfer and Fluid Flow* (Hemisphere, New York, 1980).
[28] J. P. Van Doormaal and G. D. Raithby, Numer. Heat Transfer **7**, 147 (1984).
[29] T. P. Chiang and W. H. Sheu, Comp. Mech. **20**, 379 (1997).
[30] R. Legendre, Rech. Aeronaut. **54**, 3 (1956).
[31] M. J. Lighthill, in *Laminar Boundary Layers*, edited by L. Rosenhead (Oxford University Press, Oxford, 1963), Vol. II, 2.6:72.
[32] M. Tobak and D. J. Peake, Annu. Rev. Fluid Mech. **14**, 61 (1982).